

SUMO-targeted ubiquitin ligase (STUbL) Slx5 regulates proteolysis of centromeric histone H3 variant Cse4 and prevents its mislocalization to euchromatin

Kentaro Ohkuni^a, Yoshimitsu Takahashi^a, Alyona Fulp^b, Josh Lawrimore^b, Wei-Chun Au^a, Nagesh Pasupala^c, Reuben Levy-Myers^{a,c}, Jack Warren^a, Alexander Strunnikov^d, Richard E. Baker^e, Oliver Kerscher^c, Kerry Bloom^b, and Munira A. Basrai^{a,*}

^aGenetics Branch, Center for Cancer Research, National Cancer Institute, National Institutes of Health, Bethesda, MD 20892; ^bDepartment of Biology, University of North Carolina at Chapel Hill, Chapel Hill, NC 27599; ^cBiology Department, The College of William & Mary, Williamsburg, VA 23187; ^dGuangzhou Institutes of Biomedicine and Health, Guangzhou 510530, China; ^eDepartment of Microbiology and Physiological Systems, University of Massachusetts Medical School, Worcester, MA 01655

ABSTRACT Centromeric histone H3, CENP-A^{Cse4}, is essential for faithful chromosome segregation. Stringent regulation of cellular levels of CENP-A^{Cse4} restricts its localization to centromeres. Mislocalization of CENP-A^{Cse4} is associated with aneuploidy in yeast and flies and tumorigenesis in human cells; thus defining pathways that regulate CENP-A levels is critical for understanding how mislocalization of CENP-A contributes to aneuploidy in human cancers. Previous work in budding yeast shows that ubiquitination of overexpressed Cse4 by Psh1, an E3 ligase, partially contributes to proteolysis of Cse4. Here we provide the first evidence that Cse4 is sumoylated by E3 ligases Siz1 and Siz2 in vivo and in vitro. Ubiquitination of Cse4 by the small ubiquitin-related modifier (SUMO)-targeted ubiquitin ligase (STUbL) Slx5 plays a critical role in proteolysis of Cse4 and prevents mislocalization of Cse4 to euchromatin under normal physiological conditions. Accumulation of sumoylated Cse4 species and increased stability of Cse4 in *slx5Δ* strains suggest that sumoylation precedes ubiquitin-mediated proteolysis of Cse4. Slx5-mediated Cse4 proteolysis is independent of Psh1, since *slx5Δ psh1Δ* strains exhibit higher levels of Cse4 stability and mislocalization than either *slx5Δ* or *psh1Δ* strains. Our results demonstrate a role for Slx5 in ubiquitin-mediated proteolysis of Cse4 to prevent its mislocalization and maintain genome stability.

Monitoring Editor

Orna Cohen-Fix
National Institutes of Health

Received: Dec 10, 2015

Revised: Feb 17, 2016

Accepted: Mar 3, 2016

INTRODUCTION

Centromeres are specialized chromosomal loci that are essential for faithful chromosome segregation. The kinetochore (centromeric DNA and associated proteins) provides an attachment site for

microtubules for segregation of sister chromatids during mitosis. Despite the wide divergence of centromere DNA sequences, kinetochore proteins such as centromeric histone H3 variant are evolutionarily conserved from yeast to humans (Cse4 in *Saccharomyces cerevisiae*, Cnp1 in *Schizosaccharomyces pombe*, CID in *Drosophila*, and CENP-A in mammals) and are essential for chromosome segregation (Kitagawa and Hieter, 2001; Smith, 2002; Biggins, 2013). The function of CENP-A is also evolutionarily conserved, as budding yeast Cse4 can rescue a depletion of mammalian CENP-A (Wieland *et al.*, 2004).

Stringent regulation of CENP-A expression is essential for genome stability. Overexpression of CENP-A causes ectopic mislocalization to chromosome arms and promotes aneuploidy in humans, flies, and yeast (Scott and Sullivan, 2014). Overexpression and

This article was published online ahead of print in MBoC in Press (<http://www.molbiolcell.org/cgi/doi/10.1091/mbc.E15-12-0827>) on March 9, 2016.

*Address correspondence to: Munira A. Basrai (basrain@nih.gov).

Abbreviations used: CHX, cycloheximide; FACT, facilitates chromatin transcription/transactions; FRAP, fluorescence recovery after photobleaching; STUbL, SUMO-targeted ubiquitin ligase; SUMO, small ubiquitin-related modifier.

© 2016 Ohkuni *et al.* This article is distributed by The American Society for Cell Biology under license from the author(s). Two months after publication it is available to the public under an Attribution-Noncommercial-Share Alike 3.0 Unported Creative Commons License (<http://creativecommons.org/licenses/by-nc-sa/3.0>).

"ASCB®," "The American Society for Cell Biology®," and "Molecular Biology of the Cell®" are registered trademarks of The American Society for Cell Biology.

mislocalization of CENP-A are observed in many cancers and contribute to tumorigenesis in human cells (Tomonaga *et al.*, 2003; Amato *et al.*, 2009; Hu *et al.*, 2010; Li *et al.*, 2011; Wu *et al.*, 2012; Lacoste *et al.*, 2014; Athwal *et al.*, 2015). In flies, mislocalization of CID causes formation of ectopic kinetochores and leads to mitotic delays, anaphase bridges, chromosome fragmentation, aneuploidy, and lethality (Heun *et al.*, 2006). In fission yeast, overexpression of Cnp1 leads to indiscriminate deposition of Cnp1 at noncentromeric regions, resulting in growth defects and severe chromosome missegregation during mitosis and meiosis (Choi *et al.*, 2012; Castillo *et al.*, 2013; Gonzalez *et al.*, 2014). In budding yeast, mislocalization of Cse4 to euchromatin leads to chromosome segregation defects, and the extent of Cse4 mislocalization directly correlates with the level of chromosome loss (Au *et al.*, 2008). Furthermore, various pathways involving kinetochore protein Spt4 (Crotti and Basrai, 2004), histone chaperones Cac1 and Hir1 (Sharp *et al.*, 2002; Lopes da Rosa *et al.*, 2011), and chromatin remodeler Snf2 (Gkikopoulos *et al.*, 2011) act to prevent the mislocalization of Cse4.

Protein posttranslational modifications, such as ubiquitination (Kerscher *et al.*, 2006), are important for regulating steady-state levels and preventing mislocalization. For example, proteolysis of CID prevents its mislocalization to ectopic regions in flies (Heun *et al.*, 2006; Moreno-Moreno *et al.*, 2011). Proteolysis of CENP-A has also been observed in senescent human cells or upon infection with herpes simplex virus 1 (Lomonte *et al.*, 2001; Maehara *et al.*, 2010). In fission yeast, the N-terminus of Cnp1 regulates ubiquitin-mediated proteolysis of Cnp1 and prevents its mislocalization to ectopic loci (Gonzalez *et al.*, 2014). In budding yeast, ubiquitin-mediated proteolysis of Cse4 by E3 ubiquitin ligase Psh1 (Hewawasam *et al.*, 2010; Ranjitkar *et al.*, 2010) and proline isomerase Fpr3 (Ohkuni *et al.*, 2014) regulates cellular levels of Cse4. Both the N-terminus of Cse4 and the centromere-targeting domain in the C-terminus of Cse4 (which interacts with Psh1) are required for proteolysis of overexpressed Cse4 (Hewawasam *et al.*, 2010; Ranjitkar *et al.*, 2010; Au *et al.*, 2013). Psh1-mediated proteolysis of Cse4 is also affected by the facilitates chromatin transcription/transactions (FACT) complex (Deyter and Biggins, 2014) and phosphorylation of Psh1 by casein kinase 2 (Hewawasam *et al.*, 2014). Given that Cse4 is not completely stabilized in the *psh1Δ* mutant, we hypothesize that additional mechanisms regulate proteolysis of Cse4. Identification of cellular pathways for CENP-A proteolysis is critical for understanding mechanisms that prevent mislocalization of CENP-A and aneuploidy in human cancers.

In addition to ubiquitination, sumoylation is also a critical modifier of chromatin proteins, such as histone H3 (Nathan *et al.*, 2006). Sumoylation affects several biological processes, including transcription, signal transduction, and genome integrity, by regulating protein–protein or protein–DNA interactions or by localization and stability of the interacting proteins (Ulrich, 2009; Gareau and Lima, 2010; Everett *et al.*, 2013; Flotho and Melchior, 2013; Jentsch and Psakhye, 2013). A recent study showed that the interaction of CDC48/p97 with sumoylated CENP-A activates rRNA genes in *Arabidopsis thaliana* (Merai *et al.*, 2014). However, these studies did not define the sumoylation enzymes or a functional role for sumoylated CENP-A in chromosome segregation. In budding yeast, the covalent attachment of Smt3, a small ubiquitin-related modifier (SUMO), to target lysines requires the activity of E3 SUMO ligases such as Siz1 and Siz2 (Johnson and Gupta, 2001; Takahashi *et al.*, 2001). SUMO-targeted ubiquitin ligases (STUbLs) link SUMO and ubiquitin modification pathways and facilitate proteolysis of the substrate. Slx5 and Slx8, two of at least four STUbLs proteins in *S. cerevisiae*, form a heterodimer to mediate SUMO-targeted degradation of

several proteins, including Mot1 and MAT α 2 (Wang and Prelich, 2009; Xie *et al.*, 2010), nuclear Siz1 during mitosis (Westerbeck *et al.*, 2014), and proteins involved in the DNA damage response and genome maintenance (Cook *et al.*, 2009; Hickey *et al.*, 2012; Garza and Pillus, 2013; Sriramachandran and Dohmen, 2014). Slx5, but not Slx8, has been shown to associate with centromeres, and *slx5Δ* and *slx8Δ* mutants show defects in chromosome segregation (van de Pasch *et al.*, 2013). Depletion of the human homologue of Slx5/8, RNF4, also leads to chromosome segregation errors (van de Pasch *et al.*, 2013), suggesting that the role of Slx5/8 is evolutionarily conserved. The kinetochore substrates targeted and modified by Slx5/8 have not been identified, and therefore the role of STUbL proteins in chromosome segregation and genome stability is not well understood.

Here we provide evidence that Cse4 is sumoylated by SUMO E3 ligases Siz1 and Siz2 *in vivo* and *in vitro* and that SUMO modification of Cse4 regulates its proteolysis. Slx5 plays a critical role in ubiquitin-mediated proteolysis of Cse4 and prevents mislocalization of Cse4 under normal physiological conditions. Mislocalized Cse4 is highly stable and is not efficiently degraded in *psh1Δ* and *slx5Δ* strains. Our results show that Slx5 regulates ubiquitin-mediated proteolysis of Cse4 to prevent its mislocalization in a Psh1-independent manner.

RESULTS

Cse4 is sumoylated *in vitro* and *in vivo*

Protein posttranslational modifications such as ubiquitination and sumoylation are important for regulating steady-state levels of cellular proteins (Kerscher *et al.*, 2006; Everett *et al.*, 2013). Although canonical histones are sumoylated (Nathan *et al.*, 2006), there is no evidence for sumoylation of Cse4. Optimization of the biochemical purification of Cse4 allowed us to detect sumoylation of Cse4 *in vivo*. We performed a pull down of octahistidine-hemagglutinin (8His-HA)-tagged Cse4 using nickel-nitrilotriacetic acid (Ni-NTA) agarose beads and detected SUMO-modified Cse4 by Western blot analysis with an anti-Smt3 antibody (Figure 1A). Protein levels of *cse4* 16KR, in which all lysine (K) residues are mutated to arginine (R), were greatly increased due to its stabilization, as reported previously (Collins *et al.*, 2004). At least three high-molecular weight bands were observed after transient overexpression of 8His-HA-Cse4 in wild-type cells (Figure 1A, long exposure, denoted by arrows). In contrast, these SUMO-modified Cse4 species, which are visible on wild-type 8His-HA-Cse4, were not detected with vector alone or 8His-HA-*cse4* 16KR. These results show that Cse4 is sumoylated *in vivo*.

To identify the SUMO E3 ligase responsible for Cse4 sumoylation, we tested the role of two functionally redundant SUMO E3 ligases, Siz1 and Siz2, that are responsible for sumoylation of a majority of substrates (Johnson and Gupta, 2001; Johnson, 2004; Takahashi *et al.*, 2001; Montpetit *et al.*, 2006; Reindle *et al.*, 2006), including the kinetochore protein Ndc10 and histones H2B and H4 in *S. cerevisiae* (Montpetit *et al.*, 2006; Nathan *et al.*, 2006). *In vitro* sumoylation assays using purified Cse4 (Supplemental Figure S1) revealed that Siz1 serves as an E3 for Cse4 sumoylation (Figure 1B). We tested a *siz1Δ siz2Δ* mutant to determine the role of Siz1 and Siz2 in sumoylation of Cse4 *in vivo* (Figure 1C). We failed to detect SUMO-modified Cse4 species in the *siz1Δ siz2Δ* strain compared with the wild-type strain (Figure 1C, pull down). The lower levels of input Cse4 in the *siz1Δ siz2Δ* strain may be due to their slow growth and/or a defect in transcriptional induction from the GAL promoter (Figure 1C, input); however, SUMO-modified Cse4 species were not detected in the *siz1Δ siz2Δ* strain even upon a longer exposure

(Figure 1C, long exposure). Our results show that SUMO E3 ligases Siz1 and Siz2 sumoylate Cse4 *in vivo*.

The STUbL Slx5 regulates ubiquitin-mediated proteolysis of Cse4

Previous studies showed that STUbLs link SUMO and ubiquitin modification pathways to facilitate proteolysis of cellular substrates (Garza and Pillus, 2013; Sriramachandran and Dohmen, 2014). Slx5, one of four STUbL proteins (Slx5, Slx8, Uls1, Rad18) in *S. cerevisiae*, forms a complex with Siz1 (Westerbeck *et al.*, 2014), and *slx5Δ* strains exhibit chromosome segregation defects (van de Pasch *et al.*, 2013). Hence we investigated the role of Slx5 in Cse4 proteolysis. To investigate whether Slx5 interacts with Cse4 *in vivo*, we performed a glutathione S-transferase (GST) pull-down assay using a strain expressing GST-tagged Slx5 and HA-tagged Cse4. Slx5-GST was affinity purified on glutathione sepharose, and copurifying HA-Cse4 was detected by Western blot analysis with anti-HA antibody (Figure 2A). Our results show that GST-Slx5 interacts with HA-Cse4 *in vivo*.

To determine whether Slx5 ubiquitinates Cse4 *in vivo*, we performed an affinity pull-down assay using agarose with tandem ubiquitin-binding entities (Ub*) from a strain expressing HA-tagged Cse4 (Figure 2B). Ubiquitinated Cse4 was detected as a laddering pattern in wild-type cells expressing HA-Cse4 but was absent in strains with vector alone. Faster-migrating Cse4 species (Figure 2B, asterisk) similar in size to those in the input lane were observed from both wild-type and *slx5Δ* strains. These species were also observed in experiments with wild-type Cse4 and *cse4 16KR* mutant, in which all lysines are mutated to arginines (Au *et al.*, 2013; Hewawasam *et al.*, 2014). Because *cse4 16KR* cannot be ubiquitinated, this faster-migrating species represents unmodified Cse4, which likely interacts with ubiquitinated proteins such as canonical histones. The laddering pattern of higher-molecular weight forms of Cse4 was greatly reduced in a *slx5Δ* strain (Figure 2B). Quantification of ubiquitinated Cse4 showed a fivefold reduction in high-molecular weight forms of Cse4 when normalized to input Cse4 in the *slx5Δ* strain (Figure 2C). We next investigated whether defects in Cse4 ubiquitination result in increased protein stability *in vivo*. Overexpressed HA-tagged Cse4 was transiently induced from a *GAL* promoter by the addition of galactose, and cells were shifted to glucose medium containing cycloheximide (CHX) to inhibit translation. Western blot analysis with protein extracts from different time points was used to measure levels of Cse4 after CHX treatment (Figure 2D). HA-Cse4 was rapidly degraded in the wild-type strain ($t_{1/2} = 39.0$ min) yet was stabilized in the *slx5Δ* strain ($t_{1/2} = 73.2$ min). Consistent with this observation, we detected a similar stabilization of Cse4 in the *siz1Δ siz2Δ* strain ($t_{1/2} = 74.8$ vs. 35.8 min in wild type; Supplemental Figure S2). Thus we conclude that Slx5 is required for ubiquitination and proteolysis of Cse4 *in vivo*.

Because *slx5Δ* strains show defects in Cse4 ubiquitination and increased stability of Cse4, we examined whether sumoylated Cse4 accumulates in these strains. We first constructed a strain expressing His-Flag-tagged Smt3 (HF-Smt3) and Myc-tagged Cse4. HF-Smt3 was purified from cell extracts using Ni-NTA agarose beads, and the level of sumoylated proteins and sumoylated Cse4 was determined using anti-Flag (Smt3) and anti-Myc (Cse4) antibodies, respectively. When Myc-Cse4 was transiently overexpressed, SUMO-modified Cse4 species were barely detectable in the wild-type strain (Figure 2E, α -Myc). In contrast, the *slx5Δ* strain showed substantial levels of sumoylated Cse4, especially high-molecular weight, SUMO-modified Cse4 (Figure 2E, α -Myc). Therefore reduced STUbL activity in *slx5Δ* strain contributes to the accumulation of sumoylated Cse4

species, suggesting that Slx5-mediated proteolysis is a downstream consequence of Cse4 sumoylation.

We next examined whether higher levels of sumoylated Cse4 species accumulate in the *slx5Δ* strain under normal physiological conditions. Even though sumoylated Cse4 species were detected in wild-type cells when Cse4 is overexpressed (Figure 1A), we failed to detect sumoylated Cse4 species in the wild-type strain when Cse4 is expressed from its own promoter (Figure 2F). The failure to detect sumoylated Cse4 species may be due to low Cse4 expression and/or ongoing proteolysis of sumoylated Cse4. In contrast, higher levels of sumoylated Cse4 species were clearly observed in the *slx5Δ* mutant (Figure 2F, arrows). A defect in STUbL activity may in part contribute to accumulation of polysumoylated (high-molecular weight) Cse4 species in the *slx5Δ* strain. Sumoylated Cse4 does not accumulate in strains deleted for *PSH1*, an E3-ubiquitin ligase targeting Cse4, or in *SIZ1/SIZ2*-deleted strains. These results indicate that lack of STUbL activity in *slx5Δ* strains contributes to the accumulation of sumoylated Cse4 species under normal physiological conditions.

Slx5 regulates ubiquitin-mediated proteolysis of Cse4 in a Psh1-independent manner

Previous studies showed that Psh1 interacts with Cse4 and *CSE4* overexpression causes growth inhibition in a *psh1Δ* strain (Hewawasam *et al.*, 2010; Ranjitkar *et al.*, 2010). Similar to the growth defect observed for *psh1Δ* strains, *slx5Δ* and *siz1Δ siz2Δ* strains also showed growth inhibition with *GAL-CSE4* on galactose medium (Supplemental Figure S3). Given that Slx5 and Psh1 are E3 ligases that ubiquitinate Cse4 and that deletion of *SLX5* results in accumulation of sumoylated Cse4 species, we examined whether Slx5-mediated proteolysis of Cse4 is dependent on Psh1. We constructed *psh1Δ slx5Δ* strains using standard yeast mating and sporulation. The *psh1Δ slx5Δ* strains do not exhibit growth defects at 30°C but exhibit a slow-growth phenotype at low (22, 25°C) and high (37°C) temperatures compared with each single mutant (Supplemental Figure S4A). The *psh1Δ slx5Δ* strains also exhibit sensitivity to growth on benomyl (microtubule-depolymerizing agent)-containing plates. Furthermore, *psh1Δ slx5Δ* strains exhibit defects in segregation of a reporter chromosome in a colony color assay to measure chromosome transmission fidelity (Supplemental Figure S4B).

We next analyzed the stability of Cse4 after transient overexpression of HA-Cse4 in wild-type, *psh1Δ*, *slx5Δ*, and *psh1Δ slx5Δ* strains (Figure 3A). As expected, deletion of *PSH1* or *SLX5* moderately stabilized HA-Cse4 protein levels. In contrast, the double-deletion mutant *psh1Δ slx5Δ* showed a dramatic increase in HA-Cse4 protein stability. The half-life of HA-Cse4 in *psh1Δ slx5Δ* ($t_{1/2} = 138.6$ min) is twice that of *psh1Δ* ($t_{1/2} = 77.0$ min) or *slx5Δ* ($t_{1/2} = 69.3$ min) strains (Figure 3B). We next analyzed Cse4 stability in strains expressing HA-Cse4 from its own promoter. Protein stability assays showed that Cse4 is rapidly degraded in wild-type cells ($t_{1/2} = 34.7$ min), modestly stable in *psh1Δ* ($t_{1/2} = 46.2$ min) and *slx5Δ* ($t_{1/2} = 53.3$ min) single mutants, and highly stable in *psh1Δ slx5Δ* strain ($t_{1/2} = 77.0$ min; Figure 3, C and D). We conclude that Slx5 regulates ubiquitin-mediated proteolysis of Cse4 independently of Psh1.

Slx5 prevents mislocalization of Cse4 in a Psh1-independent manner

We investigated the physiological consequence of defects in STUbL activity by analyzing Cse4 localization in strains expressing Cse4 from its endogenous promoter. Subcellular fractionation and chromosome spreads were used to examine whether Cse4 was

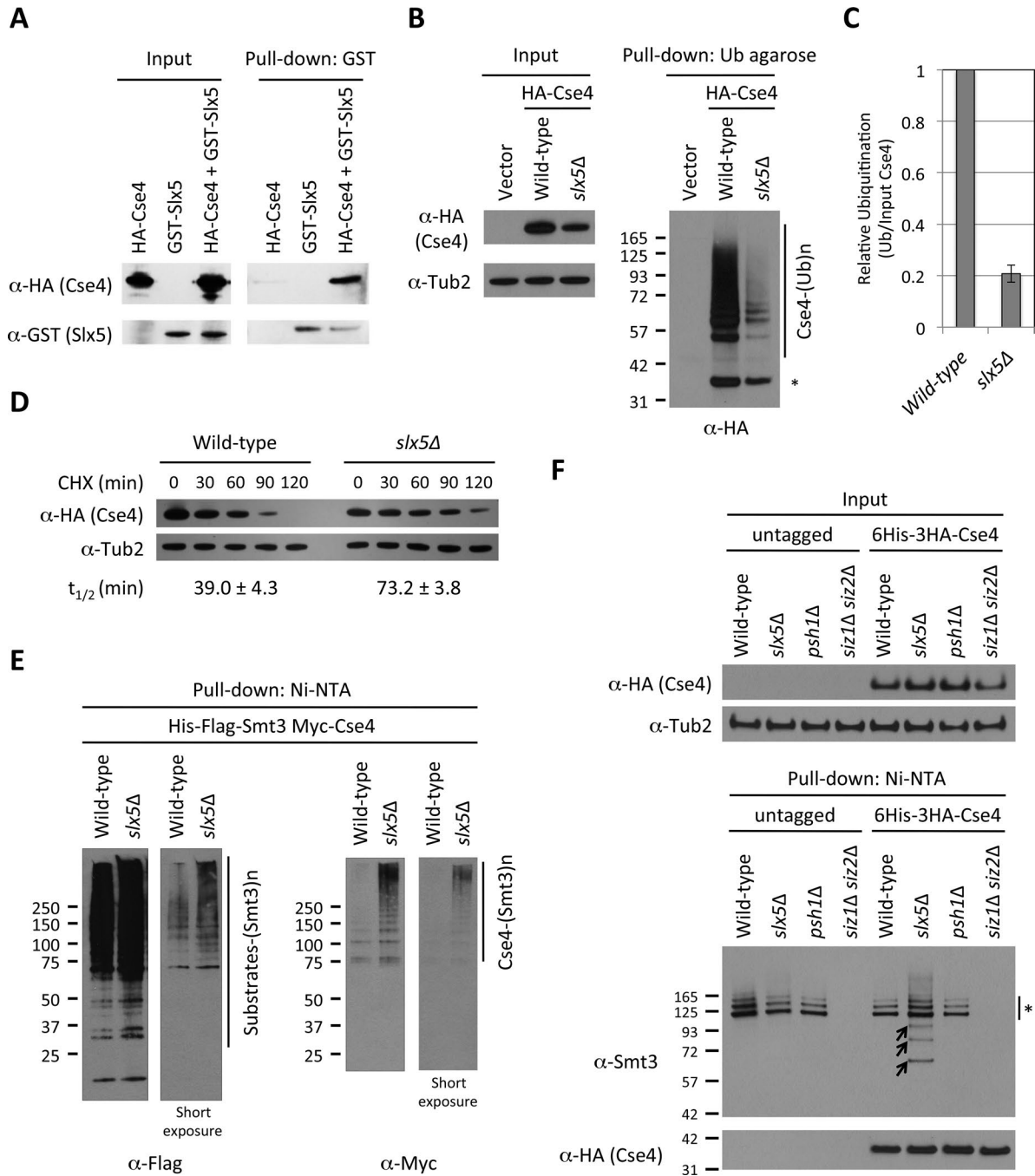


FIGURE 2: The STUbl Slx5 interacts with Cse4 and regulates ubiquitin-mediated proteolysis of Cse4. (A) Slx5 associates with Cse4. Expression of *pGAL-3HA-CSE4* (pMB1515) and/or *pGAL-GST-SLX5* (BOK629) in *ubc4* Δ *ubc6* Δ (YOK2501) was induced by the addition of galactose (2%) for 6 h. Glutathione–Sepharose beads were used for GST-Slx5 pull down, and the eluate was analyzed by Western blot analysis with anti-HA (Cse4) and anti-GST (Slx5) antibodies. (B) Slx5 regulates Cse4 ubiquitination. Wild-type (BY4741) and *slx5* Δ (YMB9035) strains expressing *pGAL-3HA-CSE4* (pMB1597) were grown in raffinose/galactose (2%) for 2 h. Agarose-TUBE1 was used for pull down with tandem ubiquitin-binding entities. Ubiquitination levels of Cse4 were detected by Western blot analysis with anti-HA antibody, and input samples were analyzed using anti-HA (Cse4) and anti-Tub2 antibodies. Wild-type (BY4741) strain transformed with vector (pMB433) was used as a negative control. Asterisk shows nonmodified Cse4. (C) Relative ubiquitination of Cse4 with average deviation of two biological repeats. Cse4 was normalized using input Cse4 levels. (D) Increased stability of Cse4 in *slx5* Δ strain. Cse4 expression from *pGAL-6His-3HA-CSE4* (pMB1458) in wild-type (BY4741) and *slx5* Δ (YMB9035) strains was induced by the addition of galactose (2%) for 2 h. Glucose (2%) containing CHX (10 μ g/ml) was added, and cells were collected at the indicated time points. Blots were probed with anti-HA (Cse4) or anti-Tub2 (loading control) antibody. Cse4 protein half-life ($t_{1/2}$) represents the mean of two biological repeats with average deviation. (E) Deletion of *SLX5* shows an accumulation of sumoylated Cse4 species. Wild-type (YMB7278) and *slx5* Δ (YMB7875) strains expressing *pGAL-13Myc-CSE4* (pSB816) were grown in raffinose/galactose (2%) for 4 h. His-Flag–tagged Smt3 (HF-Smt3) was pulled down by Ni-NTA agarose beads. Cellular levels of sumoylated proteins and sumoylated Cse4 were detected by

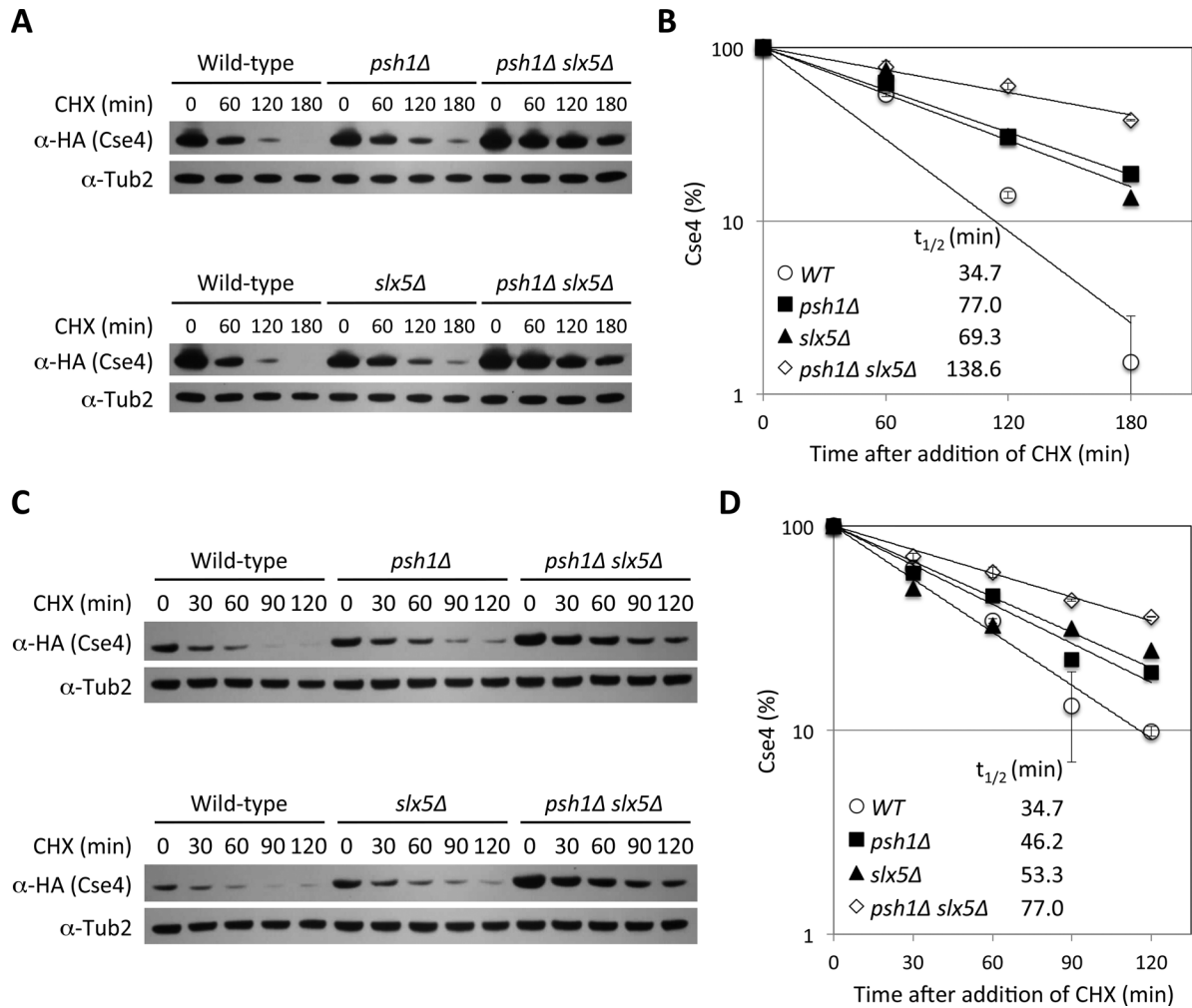


FIGURE 3: Slx5 regulates Cse4 proteolysis in a Psh1-independent manner. (A) Cse4 expressed from galactose-inducible promoter is highly stable in *psh1Δ slx5Δ* strain. Wild-type (BY4741), *psh1Δ* (YMB9034), *slx5Δ* (YMB9035), and *psh1Δ slx5Δ* (YMB9040) strains expressing *pGAL-6His-3HA-CSE4* (pMB1458) were assayed as described in Figure 2D. (B) Kinetics of turnover from A. Cse4 protein half-life ($t_{1/2}$) is indicated. Error bars in wild type and *psh1Δ slx5Δ* represent average deviation of two replicates. (C) Cse4 expressed from its own promoter is moderately stabilized in *psh1Δ* and *slx5Δ* strains and highly stable in *psh1Δ slx5Δ* strain. Protein extracts were prepared from cells grown to logarithmic phase in YPD, treated with CHX (20 μ g/ml) for various time points, and analyzed by Western blot analysis with anti-HA (Cse4) or anti-Tub2 (loading control) antibody. Isogenic yeast strains used are wild type (YMB7290), *psh1Δ* (YMB7393), *slx5Δ* (YMB7588), and *psh1Δ slx5Δ* (YMB7607). (D) Kinetics of turnover from C. Cse4 protein half-life ($t_{1/2}$) is indicated, and error bars in wild-type and *psh1Δ slx5Δ* strains represent average deviation of two replicates.

mislocalized in the *slx5Δ* strain. These approaches were previously used to show that defects in ubiquitin-mediated proteolysis of Cse4 in a *psh1Δ* strain led to the enrichment of Cse4 in chromatin and mislocalization to euchromatin when Cse4 was overexpressed (Hewawasam *et al.*, 2010; Ranjitkar *et al.*, 2010; Deyter and Biggins, 2014). Subcellular fractionation of whole-cell lysates was performed with *psh1Δ*, *slx5Δ*, and *psh1Δ slx5Δ* strains. Cse4 was barely detectable in the chromatin fraction in a wild-type strain, as its localization

is restricted to centromeres (Figure 4A). In contrast, Cse4 was enriched in chromatin in *psh1Δ* and *slx5Δ* strains, and this enrichment was further enhanced in *psh1Δ slx5Δ* strains. Similar results were observed for chromatin enrichment of Cse4 transiently overexpressed from a *GAL* promoter in *psh1Δ* and *slx5Δ* strains, with maximum enrichment in the *psh1Δ slx5Δ* strain (Supplemental Figure S5). These results suggest that Slx5 regulates localization of Cse4 independently of Psh1.

Western blot analysis with anti-Flag (Smt3) and anti-Myc (Cse4) antibodies, respectively. Two different exposures are shown. (F) Deletion of *SLX5*, but not *PSH1*, shows an accumulation of sumoylated Cse4 expressed from its own promoter. Protein extracts were prepared from cells grown to logarithmic phase in YPD. Sumoylation levels of Cse4 and nonmodified Cse4 were detected using Ni-NTA pull down, followed by Western blot analysis with anti-Smt3 and anti-HA (Cse4) antibodies, respectively. Input samples were analyzed using anti-HA (Cse4) and anti-Tub2 antibodies. At least three high molecular weights of 6His-3HA-Cse4 (arrows) were detected in the *slx5Δ* strain. Asterisk shows nonspecific sumoylated proteins that bind to the beads. Isogenic yeast strains used are wild type (YMB7290), *slx5Δ* (YMB7588), *psh1Δ* (YMB7393), and *siz1Δ siz2Δ* (YMB7611) and untagged strains (BY4742, YMB9034, YMB9035, YMB7277).

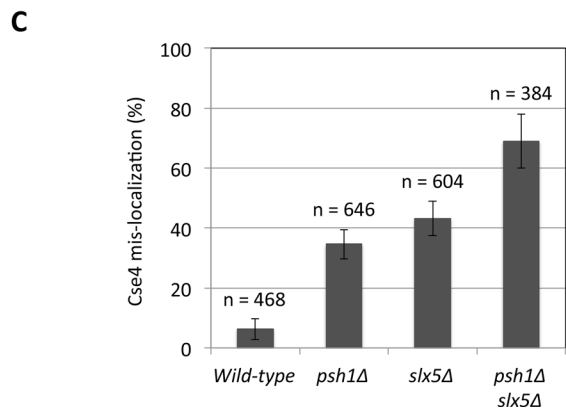
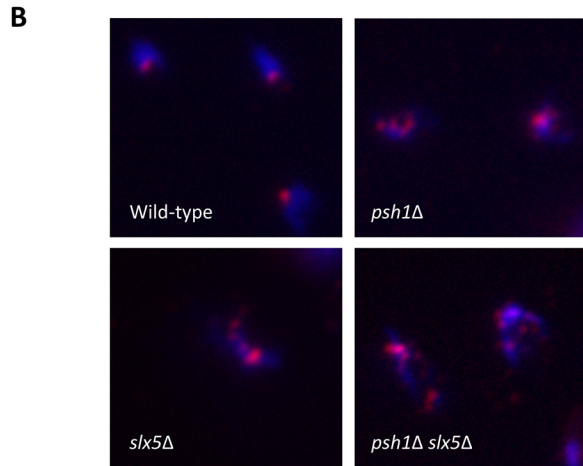
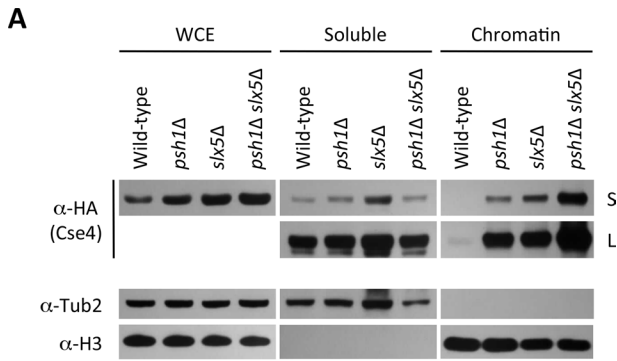


FIGURE 4: Slx5 prevents mislocalization of Cse4 to euchromatin. (A) Cse4 expressed from its own promoter is increased in chromatin fraction in *psh1Δ*, *slx5Δ*, and *psh1Δ slx5Δ* strains. Whole-cell extracts (WCEs) prepared from equal numbers of logarithmically growing cells in YPD were fractionated into soluble and chromatin fraction and assayed by Western blot analysis. Tub2 and histone H3 were used as markers for soluble and chromatin fractions, respectively. Two blots shown for Cse4 are indicated (L, long exposure; S, short exposure). (B, C) Cse4 expressed from its own promoter is mislocalized in *psh1Δ*, *slx5Δ*, and *psh1Δ slx5Δ* strains. Chromosome spreads were done by logarithmically growing cells in YPD. DAPI (blue) and α -HA (red) staining were used to visualize DNA and Cse4 localization, respectively. In wild-type strains, Cse4 is predominantly localized to one or two kinetochore clusters. In mutant strains, mislocalization of Cse4 is observed as multiple foci or diffused localization throughout the nucleus. The graph quantifies the number of cells exhibiting Cse4 mislocalization, and error bars are average deviation of two independent experiments. The number of cells used is indicated (*n*). Isogenic yeast strains used are wild type (YMB7290), *psh1Δ* (YMB7393), *slx5Δ* (YMB7588), and *psh1Δ slx5Δ* (YMB7607).

We next used chromosome spreads, a technique that removes soluble material to visualize localization of chromatin-bound Cse4 in wild-type, *psh1Δ*, *slx5Δ*, and *psh1Δ slx5Δ* strains expressing Cse4 from own promoter (Figure 4B). In wild-type cells, Cse4 foci were restricted to one or two dots, which correspond to kinetochore clusters. In contrast, diffused or multiple foci of Cse4 that overlapped with the 4',6-diamidino-2-phenylindole (DAPI)-stained nucleus were observed in *psh1Δ* and *slx5Δ* strains, and this was further exacerbated in *psh1Δ slx5Δ* cells (Figure 4, B and C). On the basis of these results, we conclude that Slx5 and Psh1 prevent mislocalization of Cse4 under normal physiological conditions and that Slx5 regulates localization of Cse4 in a Psh1-independent manner.

Fluorescence recovery after photobleaching analysis shows that mislocalized Cse4 is highly stable in *psh1Δ* and *slx5Δ* strains

To determine whether the euchromatic pool of mislocalized Cse4 observed in chromosome spreads of *slx5Δ* and *psh1Δ* strains is stably incorporated, we performed fluorescence recovery after photobleaching (FRAP) in both mutants. In wild-type strains, Cse4-GFP signal is restricted to the cluster of 16 kinetochores proximal to the spindle pole body, and Cse4 incorporated into kinetochores does not recover after photobleaching (Pearson *et al.*, 2004). In addition to the kinetochore signal (foci), the nuclei of *slx5Δ* and *psh1Δ* strains show a diffuse fluorescence emanating from noncentromeric regions (haze), consistent with the increased levels of Cse4 in chromatin fractions (Figure 4A) and mislocalization to euchromatin (Figure 4B). Similar to wild-type cells, the centromere Cse4-GFP foci in both *slx5Δ* and *psh1Δ* cells did not exhibit recovery after photobleaching (Figure 5, A and B). We next examined FRAP of the Cse4-GFP haze in *slx5Δ* and *psh1Δ* strains. For *psh1Δ* strains, we imaged Cse4-GFP haze every 30 s postbleach (Figure 5, B and D); however, because the Cse4-GFP haze was dimmer in *slx5Δ*, we used only two Z-series (immediately postbleach and 5 min postbleach) after laser bleaching to minimize photobleaching from imaging (Figure 5, A and C). Similar to the centromere Cse4-GFP foci, the Cse4-GFP haze did not exhibit recovery after photobleaching in either *slx5Δ* or *psh1Δ* cells (Figure 5, C and D). We conclude that the ectopically localized Cse4 present in *slx5Δ* and *psh1Δ* cells, once deposited, is stable.

DISCUSSION

In this study, we showed that sumoylation and ubiquitination of Cse4 regulate its proteolysis and prevent its mislocalization. We provide the first evidence for sumoylation of Cse4, by SUMO E3 ligases Siz1 and Siz2 *in vivo* and *in vitro*, and define a role for Slx5 in ubiquitin-mediated proteolysis of Cse4. Slx5-mediated proteolysis of Cse4 is independent of Psh1, and Cse4 is mislocalized to euchromatin in both *psh1Δ* and *slx5Δ* strains under normal physiological conditions. Consistent with these results, Cse4 is highly enriched in the chromatin fraction and stably incorporated into euchromatin in *psh1Δ* and *slx5Δ* strains. Taken together, our results support a role for Slx5 in ubiquitination of sumoylated Cse4 to regulate its proteolysis and localization.

Several lines of evidence support the role of Slx5 in proteolysis of Cse4. Overexpression of *CSE4* results in growth inhibition in *slx5Δ* and *siz1Δ siz2Δ* strains, similar to *psh1Δ* strain (Hewawasam *et al.*, 2010; Ranjitkar *et al.*, 2010; Au *et al.*, 2013). Second, defects in Cse4 ubiquitination observed in *slx5Δ* strains correlate with an increased half-life of Cse4 in these strains. Higher stability of Cse4 is also observed in an *slx8Δ* strain (unpublished data), suggesting that the heterodimeric Slx5/8 STUBL complex is important for Cse4 proteolysis. Third, deletion of *SLX5* leads to accumulation of higher-molecular

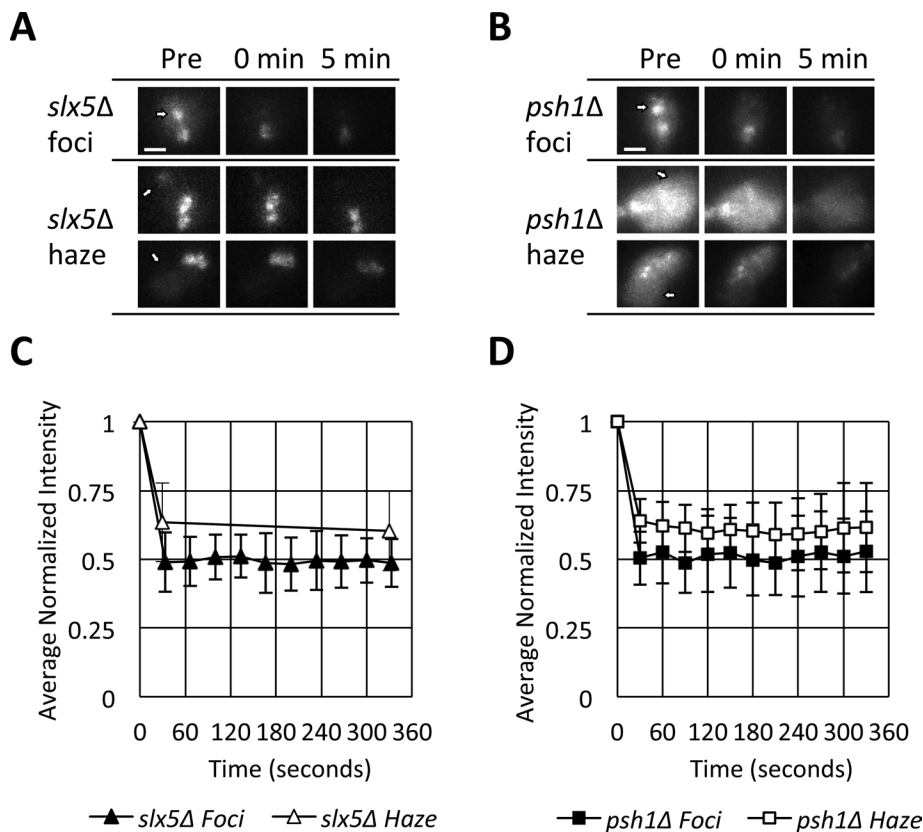


FIGURE 5: Cse4 is stable in euchromatin in *slx5Δ* and *psh1Δ* strains. Representative images of *slx5Δ* (A) and *psh1Δ* (B) cells containing Cse4-GFP before (Pre), immediately after (0 min), and 5 min after photobleaching. Foci correspond to Cse4-GFP enrichment at centromeres. Haze corresponds to Cse4-GFP at euchromatin. Arrows indicate bleached area. Images were compiled using maximum projection. Scale bar, 1 μ m. Plots of average normalized intensity of the bleached area over time for *slx5Δ* (C) and *psh1Δ* (D). Integrated intensity was background subtracted and corrected for photobleaching. Error bars show SD. Bleaching was set at $t = 30$ s. For *slx5Δ*, nine cells were used each for foci and haze, and for *psh1Δ*, eight cells each for foci and haze. Isogenic yeast strains used are *slx5Δ* (YMB9429) and *psh1Δ* (YMB9430).

weight species of sumoylated Cse4. Similar results for higher levels of sumoylated Mot1, a regulator of TATA-binding protein and defects in proteolysis, were observed when *SLX5* and/or *SLX8* are deleted (Wang and Prelich, 2009). Accumulation of sumoylated Cse4 species and increased stability of Cse4 in the *slx5Δ* strain suggest that sumoylation precedes ubiquitin-mediated proteolysis of Cse4. These phenotypes are not limited to cases in which Cse4 is overexpressed (e.g., using the *GAL* promoter); higher levels of sumoylated Cse4 and increased stability of Cse4 are also observed under physiological conditions when Cse4 is expressed from its own promoter.

The increased stability of Cse4 in the *psh1Δ slx5Δ* double mutant compared with either the *slx5Δ* or *psh1Δ* single mutant shows that Slx5-mediated proteolysis of Cse4 is independent of Psh1 under normal physiological conditions. The residual proteolysis of Cse4 observed in *psh1Δ slx5Δ* strains suggests that additional pathways/regulators that have yet to be identified also mediate Cse4 proteolysis. This is perhaps not surprising, given that degradation of excess of histone H3 is also regulated by at least five E3 ubiquitin ligases (Singh et al., 2012). In addition, non-ubiquitin-mediated pathways partially contribute to Cse4 proteolysis because mutant *cse4* 16KR, in which all lysines are changed to arginine, is still degraded (Collins et al., 2004; Au et al., 2013).

Endogenously expressed Cse4 is enriched in chromatin fractions and mislocalized to euchromatin in *slx5Δ* and *psh1Δ* strains, and

these phenotypes are further exacerbated in the *slx5Δ psh1Δ* double mutant. Previous studies examined Cse4 turnover only in the context of the kinetochore, where it is stably incorporated into chromatin (Pearson et al., 2004). Although the signal is low, the increased levels of noncentromeric Cse4 present in *slx5Δ* and *psh1Δ* strains (the "haze") enable analysis by FRAP. The apparent stability of mislocalized Cse4 observed by FRAP suggests that ectopically localized Cse4 is stably incorporated in the euchromatin; however, it is also possible that the ectopic Cse4-containing nucleosomes are dynamic, in equilibrium with (non-fluorescently tagged) H3 in the nucleus (Verdaasdonk et al., 2012). The latter explanation would require that the exchange mechanism uses a different Cse4/H3 pool than that under which the Cse4 was initially misincorporated.

We propose a model (Figure 6) in which sumoylation and ubiquitination regulate Cse4 proteolysis to prevent its stable incorporation into euchromatin. At least two independent pathways regulate Cse4 proteolysis. One is dependent on the interaction of Psh1 with Cse4, which is potentiated by the nucleosome-destabilizing activity of the FACT complex. This suggests that Psh1 is primarily responsible for removing nucleosomal Cse4 at noncentromeric chromatin, even though the interaction of Psh1 and soluble Cse4 is also reduced in the absence of FACT (Deyter and Biggins, 2014). The second pathway, identified here, requires sumoylation of Cse4 by Siz1/Siz2 and subsequent ubiquitination of Cse4 by Slx5 to regulate cellular levels of Cse4 and prevent its mislocalization to euchromatin. Although we do not yet know whether the Siz1/2-Slx5 pathway acts on soluble Cse4 or chromatin-bound Cse4, together the two pathways act to regulate cellular levels of Cse4 and prevent its mislocalization to euchromatin. Given that mislocalization of Cse4 leads to chromosome segregation defects, it is not surprising that cells use multiple ubiquitination pathways for proteolysis of high levels of Cse4.

Unlike Psh1, Slx5 and Slx8 are evolutionarily conserved, and depletion of the human STUbL orthologue, RNF4, results in defects in chromosome segregation (van de Pasch et al., 2013). Similar to Slx5, it is possible that RNF4 also regulates the localization of CENP-A and that defects in this pathway lead to chromosome missegregation. Previous studies showed that mislocalization of centromeric histone H3 variants Cse4, Cnp1, and CID contribute to chromosome segregation defects in flies and budding/fission yeast (Heun et al., 2006; Au et al., 2008; Gonzalez et al., 2014). Thus we propose that the mislocalization of CENP-A contributes to chromosome segregation defects in *slx5Δ* and RNF4-depleted cells. These studies are important, as we do not fully understand how overexpression and mislocalization of CENP-A observed in many cancers contribute to tumorigenesis. Our studies on the role of STUbLs in ubiquitin-mediated proteolysis of Cse4 provide mechanistic insights into pathways that prevent mislocalization of CENP-A and aneuploidy in human cancers.

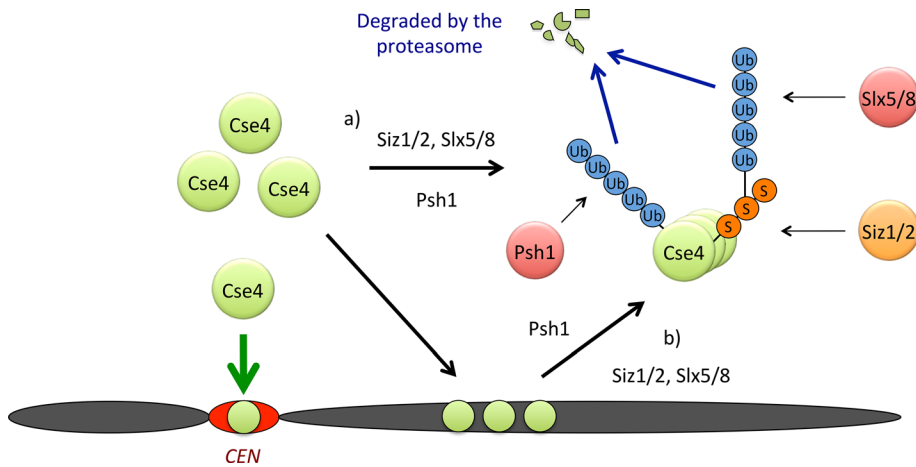


FIGURE 6: Model for how Slx5 regulates proteolysis of Cse4 and prevents its mislocalization to euchromatin. Restricting the localization of Cse4 to centromeric DNA is essential for faithful chromosome segregation. At least two independent pathways prevent the stable incorporation of Cse4 into euchromatin. One of these pathways is dependent on the interaction of Psh1 with Cse4. The second pathway requires sumoylation of Cse4 by Siz1/Siz2 and ubiquitination of sumoylated Cse4 by Slx5. The two pathways may a) regulate soluble pools of Cse4 to prevent its mislocalization and/or b) facilitate proteolysis of chromatin-bound Cse4.

MATERIALS AND METHODS

Yeast strains and plasmids

Supplemental Tables S1 and S2 describe the genotype of yeast strains and plasmids used for this study, respectively.

Sumoylation assay in vivo and in vitro

In vivo sumoylation was assayed in crude yeast extracts using Ni-NTA agarose beads to pull down His-HA-tagged Cse4 or His-Flag-tagged Smt3 (HF-Smt3) under denaturing condition, as described previously (Ohkuni *et al.*, 2015). In vitro sumoylation assays were carried out as described previously (Takahashi *et al.*, 2003). Briefly, the components of the conjugation reaction—Smt3gg, GST-Uba2, GST-Aos1, Ubc9, and Siz1- Δ 440 proteins—were expressed and purified from *Escherichia coli* and then used in the reaction mixture containing Cse4 as a substrate. Cse4 was produced in *E. coli* and purified by Sephacryl-S200 chromatography as described (Luger *et al.*, 1997). Substrate (Cse4), E1 (GST-Uba2, GST-Aos1), E2 (Ubc9), and SUMO (Smt3gg) were incubated in a total volume 20 μ l for 60 min in the presence of 10 mM ATP, 50 mM Tris-HCl (pH 8.0), 5 mM MgCl₂, and 2 mM dithiothreitol at 37°C. The reaction was stopped by adding 2 \times Laemmli buffer.

Protein stability and ubiquitin pull-down assays

Protein stability assay was performed as described previously (Ohkuni *et al.*, 2014) with some modifications. Cells were grown to logarithmic phase of growth in a 2% raffinose synthetic complete medium at 25°C. Galactose was added to the medium to a final concentration of 2% to induce Cse4 expression from the GAL promoter for 2 h at 25°C. CHX and glucose were then added to final concentrations of 10 μ g/ml and 2%, respectively. Samples were taken at the indicated time points, and levels of Cse4 were quantified by Western blot analysis. Protein levels at each time point were quantified using Gene Tools software (version 3.8.8.0) from SynGene (Frederick, MD). Ubiquitin pull-down assays were performed by inducing HA-tagged Cse4 from a GAL promoter by the addition of galactose (2%) for 2 h, as described previously (Au *et al.*, 2013).

GST pull-down assay

The *ubc4 Δ ubc6 Δ* (YOK 2501) strain was transformed with *pGAL-GST-SLX5* (BOK 629, Open Biosystems Yeast GST Collection YSC4515202484078), *pGAL-3HA-CSE4* (pMB 1515), or both *pGAL-GST-SLX5* and *pGAL-3HA-CSE4*. Transformants were grown in appropriate selective medium with proline as nitrogen source and 2% sucrose to logarithmic phase, and then 2% galactose and 0.003% SDS were added to the cultures and incubation continued for another 6 h. MG132, 75 μ M, was added 1/2 h before harvesting of the cells. We assayed 200 OD units of yeast cells as described previously (Westerbeck *et al.*, 2014). Whole-cell extracts (2 OD) and pull down (20 OD) were analyzed by Western blot analysis.

Subcellular fractionation and chromosome spreads

Subcellular fractionation to assay chromatin enrichment of Cse4 was performed as described previously (Au *et al.*, 2008). Cells were grown to logarithmic phase of growth in 1% yeast extract, 2% bactopectone, and 2% glucose (YPD) at 25°C. Chromosome spreads were performed as described previously (Collins *et al.*, 2004; Crotti and Basrai, 2004) with some modifications. 16B12 mouse anti-HA antibody (MMS-101P; Covance, Emeryville, CA) was used as primary antibody at 1:2500 dilution. Cy3-conjugated goat anti-mouse (115165003; Jackson ImmunoResearch Laboratories, West Grove, PA) was used as secondary antibody at 1:5000 dilution. Cells were visualized by DAPI staining (1 μ g/ml in phosphate-buffered saline) mounted in antifade mountant (P36935; Molecular Probes, Eugene, OR). Cells were observed under an Axioskop 2 (Zeiss) fluorescence microscope equipped with a Plan-Apochromat 100 \times (Zeiss, Thornwood, NY) oil immersion lens. Image acquisition and processing were performed with the IP Lab version 3.9.9 r3 software (Scanalytics, Fairfax, VA).

Antibodies

Antibodies for experiments were as follows: rabbit polyclonal anti-Cse4 (Strunnikov laboratory), anti-Tub2 antibodies (Basrai laboratory), anti-HA (12CA5; Roche, Indianapolis, IN), anti-HA (ab9110; Abcam, Cambridge, MA), anti-myc (A-14; Santa Cruz Biotechnology, Dallas, TX), anti-GST (ab6613; Abcam), anti-Smt3 (y-84; Santa Cruz Biotechnology), and anti-H3 (ab1791; Abcam). Anti-Cse4 was used at a dilution of 1:1000, anti-HA was used at a dilution from 1:1000 to 1:10,000, anti-Tub2 and anti-Smt3 were used at 1:3000, and anti-GST and anti-H3 were used at 1:5000.

FRAP

Strains YMB9430 (Cse4-GFP, *psh1 Δ*) and YMB9429 (Cse4-GFP, *slx5 Δ*) were grown in YPD to mid logarithmic growth phase before imaging. Both YMB9430 and YMB9429 were grown at 24°C, but YMB9429 was shifted to 37°C 6 h before imaging. Cells were imaged using a Nikon Eclipse Ti wide-field inverted microscope with a 100 \times /1.49 numerical aperture Apo total internal reflection fluorescence objective (Nikon, Melville, NY) and Andor Clara charge-coupled device camera (Andor, South Windsor, CT) using Nikon NIS Elements imaging software. Photobleaching was performed with a Sapphire 488-50 CDRH laser (Coherent, Santa Clara, CA). A seven-step Z-series with

200-nm step size with 600-ms exposure time was taken before a 300-ms exposure from the laser. Immediately after the laser exposure, a 5-min time lapse with 30-s intervals with the same settings as the first Z-series was initiated. The Z-series was compiled into single images using maximum projection, and the integrated intensity of the bleached area was measured using MetaMorph 7.7 imaging software (Molecular Devices, Sunnyvale, CA). The integrated intensity of the bleached area had the integrated intensity of the cell background subtracted at each time point, and photobleaching was corrected for by determining the average bleaching rate of a nearby Cse4-GFP signal and adding back the average signal loss per Z-series. Photobleaching and background subtraction was performed using Excel (Microsoft, Redmond, WA).

Chromosome transmission fidelity

The chromosome transmission fidelity assay was performed as described previously (Spencer *et al.*, 1990; Ohkuni *et al.*, 2008). Strains were plated on synthetic medium with limiting adenine and incubated at 25°C for 4 d. Loss of the reporter chromosome results in red sectors in an otherwise white colony. Colonies that are at least half red indicate loss of the reporter chromosome in the first cell division.

ACKNOWLEDGMENTS

We thank members of the Basrai laboratory for helpful discussions and comments on the manuscript. We gratefully acknowledge Charlie Boone, Frank Holstege, and Sue Biggins for reagents and advice, Tatiana Karpova (Fluorescent Imaging Facility, National Cancer Institute) for assistance with cell biology experiments, Kathy McKinnon (Vaccine Branch FACS Core, National Cancer Institute) for assistance with FACS, and Anita Corbett, Ian Cheeseman, Michael Lichten, Tom Misteli, and Peter Kaiser for comments on the manuscript. This work was supported by the National Institutes of Health Intramural Research Program to M.B., National Science Foundation Grant MBC 1051970 to O.K., and National Institutes of Health R37 Grant GM32238 to K.B.

REFERENCES

Amato A, Schillaci T, Lentini L, Di Leonardo A (2009). CENPA overexpression promotes genome instability in pRb-depleted human cells. *Mol Cancer* 8, 119.

Athwal RK, Walkiewicz MP, Baek S, Fu S, Bui M, Camps J, Ried T, Sung MH, Dalal Y (2015). CENP-A nucleosomes localize to transcription factor hotspots and subtelomeric sites in human cancer cells. *Epigenetics Chromatin* 8, 2.

Au WC, Crisp MJ, DeLuca SZ, Rando OJ, Basrai MA (2008). Altered dosage and mislocalization of histone H3 and Cse4p lead to chromosome loss in *Saccharomyces cerevisiae*. *Genetics* 179, 263–275.

Au WC, Dawson AR, Rawson DW, Taylor SB, Baker RE, Basrai MA (2013). A novel role of the N terminus of budding yeast histone H3 variant Cse4 in ubiquitin-mediated proteolysis. *Genetics* 194, 513–518.

Biggins S (2013). The composition, functions, and regulation of the budding yeast kinetochore. *Genetics* 194, 817–846.

Castillo AG, Pidoux AL, Catania S, Durand-Dubief M, Choi ES, Hamilton G, Ekwall K, Allshire RC (2013). Telomeric repeats facilitate CENP-A(Cnp1) incorporation via telomere binding proteins. *PLoS One* 8, e69673.

Choi ES, Stralfors A, Catania S, Castillo AG, Svensson JP, Pidoux AL, Ekwall K, Allshire RC (2012). Factors that promote H3 chromatin integrity during transcription prevent promiscuous deposition of CENP-A(Cnp1) in fission yeast. *PLoS Genet* 8, e1002985.

Collins KA, Furuyama S, Biggins S (2004). Proteolysis contributes to the exclusive centromere localization of the yeast Cse4/CENP-A histone H3 variant. *Curr Biol* 14, 1968–1972.

Cook CE, Hochstrasser M, Kerscher O (2009). The SUMO-targeted ubiquitin ligase subunit Slx5 resides in nuclear foci and at sites of DNA breaks. *Cell Cycle* 8, 1080–1089.

Crotti LB, Basrai MA (2004). Functional roles for evolutionarily conserved Spt4p at centromeres and heterochromatin in *Saccharomyces cerevisiae*. *EMBO J* 23, 1804–1814.

Deyter GM, Biggins S (2014). The FACT complex interacts with the E3 ubiquitin ligase Psh1 to prevent ectopic localization of CENP-A. *Genes Dev* 28, 1815–1826.

Everett RD, Boutell C, Hale BG (2013). Interplay between viruses and host sumoylation pathways. *Nat Rev Microbiol* 11, 400–411.

Flotho A, Melchior F (2013). Sumoylation: a regulatory protein modification in health and disease. *Annu Rev Biochem* 82, 357–385.

Gareau JR, Lima CD (2010). The SUMO pathway: emerging mechanisms that shape specificity, conjugation and recognition. *Nat Rev Mol Cell Biol* 11, 861–871.

Garza R, Pillus L (2013). STUBs in chromatin and genome stability. *Biopolymers* 99, 146–154.

Gkikopoulos T, Singh V, Tsui K, Awad S, Renshaw MJ, Scholfield P, Barton GJ, Nislow C, Tanaka TU, Owen-Hughes T (2011). The SWI/SNF complex acts to constrain distribution of the centromeric histone variant Cse4. *EMBO J* 30, 1919–1927.

Gonzalez M, He H, Dong Q, Sun S, Li F (2014). Ectopic centromere nucleation by CENP-A in fission yeast. *Genetics* 198, 1433–1446.

Heun P, Erhardt S, Blower MD, Weiss S, Skora AD, Karpen GH (2006). Mislocalization of the *Drosophila* centromere-specific histone CID promotes formation of functional ectopic kinetochores. *Dev Cell* 10, 303–315.

Hewawasam GS, Mattingly M, Venkatesh S, Zhang Y, Florens L, Workman JL, Gerton JL (2014). Phosphorylation by casein kinase 2 facilitates Psh1 protein-assisted degradation of Cse4 protein. *J Biol Chem* 289, 29297–29309.

Hewawasam G, Shivaraju M, Mattingly M, Venkatesh S, Martin-Brown S, Florens L, Workman JL, Gerton JL (2010). Psh1 is an E3 ubiquitin ligase that targets the centromeric histone variant Cse4. *Mol Cell* 40, 444–454.

Hickey CM, Wilson NR, Hochstrasser M (2012). Function and regulation of SUMO proteases. *Nat Rev Mol Cell Biol* 13, 755–766.

Hu Z, Huang G, Sadanandam A, Gu S, Lenburg ME, Pai M, Bayani N, Blakely EA, Gray JW, Mao JH (2010). The expression level of HJURP has an independent prognostic impact and predicts the sensitivity to radiotherapy in breast cancer. *Breast Cancer Res* 12, R18.

Jentsch S, Psakhye I (2013). Control of nuclear activities by substrate-selective and protein-group SUMOylation. *Annu Rev Genet* 47, 167–186.

Johnson ES (2004). Protein modification by SUMO. *Annu Rev Biochem* 73, 355–382.

Johnson ES, Gupta AA (2001). An E3-like factor that promotes SUMO conjugation to the yeast septins. *Cell* 106, 735–744.

Kerscher O, Felberbaum R, Hochstrasser M (2006). Modification of proteins by ubiquitin and ubiquitin-like proteins. *Annu Rev Cell Dev Biol* 22, 159–180.

Kitagawa K, Hieter P (2001). Evolutionary conservation between budding yeast and human kinetochores. *Nat Rev Mol Cell Biol* 2, 678–687.

Lacoste N, Woolfe A, Tachiwana H, Gareau AV, Barth T, Cantaloube S, Kurumizaka H, Imhof A, Almouzni G (2014). Mislocalization of the centromeric histone variant CenH3/CENP-A in human cells depends on the chaperone DAXX. *Mol Cell* 53, 631–644.

Li Y, Zhu Z, Zhang S, Yu D, Yu H, Liu L, Cao X, Wang L, Gao H, Zhu M (2011). ShRNA-targeted centromere protein A inhibits hepatocellular carcinoma growth. *PLoS One* 6, e17794.

Lomonte P, Sullivan KF, Everett RD (2001). Degradation of nucleosome-associated centromeric histone H3-like protein CENP-A induced by herpes simplex virus type 1 protein ICP0. *J Biol Chem* 276, 5829–5835.

Lopes da Rosa J, Holik J, Green EM, Rando OJ, Kaufman PD (2011). Overlapping regulation of CenH3 localization and histone H3 turnover by CAF-1 and HIR proteins in *Saccharomyces cerevisiae*. *Genetics* 187, 9–19.

Luger K, Rechsteiner TJ, Flaus AJ, Wayne MM, Richmond TJ (1997). Characterization of nucleosome core particles containing histone proteins made in bacteria. *J Mol Biol* 272, 301–311.

Maehara K, Takahashi K, Saitoh S (2010). CENP-A reduction induces a p53-dependent cellular senescence response to protect cells from executing defective mitoses. *Mol Cell Biol* 30, 2090–2104.

Merai Z, Chumak N, Garcia-Aguilar M, Hsieh TF, Nishimura T, Schoft VK, Bindics J, Slusarz L, Arnoux S, Opravil S, *et al.* (2014). The AAA-ATPase molecular chaperone Cdc48/p97 disassembles sumoylated centromeres, decondenses heterochromatin, and activates ribosomal RNA genes. *Proc Natl Acad Sci USA* 111, 16166–16171.

Montpetit B, Hazbun TR, Fields S, Hieter P (2006). Sumoylation of the budding yeast kinetochore protein Ndc10 is required for Ndc10 spindle

- localization and regulation of anaphase spindle elongation. *J Cell Biol* 174, 653–663.
- Moreno-Moreno O, Medina-Giro S, Torras-Llort M, Azorin F (2011). The F box protein partner of paired regulates stability of *Drosophila* centromeric histone H3, CenH3(CID). *Curr Biol* 21, 1488–1493.
- Nathan D, Ingvarsdottir K, Sterner DE, Bylebyl GR, Dokmanovic M, Dorsey JA, Whelan KA, Krsmanovic M, Lane WS, Meluh PB, et al. (2006). Histone sumoylation is a negative regulator in *Saccharomyces cerevisiae* and shows dynamic interplay with positive-acting histone modifications. *Genes Dev* 20, 966–976.
- Ohkuni K, Abdulle R, Kitagawa K (2014). Degradation of centromeric histone H3 variant Cse4 requires the Fpr3 peptidyl-prolyl cis-trans isomerase. *Genetics* 196, 1041–1045.
- Ohkuni K, Abdulle R, Tong AH, Boone C, Kitagawa K (2008). Ybp2 associates with the central kinetochore of *Saccharomyces cerevisiae* and mediates proper mitotic progression. *PLoS One* 3, e1617.
- Ohkuni K, Takahashi Y, Basrai MA (2015). Protein purification technique that allows detection of sumoylation and ubiquitination of budding yeast kinetochore proteins Ndc10 and Ndc80. *J Vis Exp* 99, e52482.
- Pearson CG, Yeh E, Gardner M, Odde D, Salmon ED, Bloom K (2004). Stable kinetochore-microtubule attachment constrains centromere positioning in metaphase. *Curr Biol* 14, 1962–1967.
- Ranjitkar P, Press MO, Yi X, Baker R, MacCoss MJ, Biggins S (2010). An E3 ubiquitin ligase prevents ectopic localization of the centromeric histone H3 variant via the centromere targeting domain. *Mol Cell* 40, 455–464.
- Reindle A, Belichenko I, Bylebyl GR, Chen XL, Gandhi N, Johnson ES (2006). Multiple domains in Siz SUMO ligases contribute to substrate selectivity. *J Cell Sci* 119, 4749–4757.
- Scott KC, Sullivan BA (2014). Neocentromeres: a place for everything and everything in its place. *Trends Genet* 30, 66–74.
- Sharp JA, Franco AA, Osley MA, Kaufman PD (2002). Chromatin assembly factor I and Hir proteins contribute to building functional kinetochores in *S. cerevisiae*. *Genes Dev* 16, 85–100.
- Singh RK, Gonzalez M, Kabbaj MH, Gunjan A (2012). Novel E3 ubiquitin ligases that regulate histone protein levels in the budding yeast *Saccharomyces cerevisiae*. *PLoS One* 7, e36295.
- Smith MM (2002). Centromeres and variant histones: what, where, when and why? *Curr Opin Cell Biol* 14, 279–285.
- Spencer F, Gerring SL, Connelly C, Hieter P (1990). Mitotic chromosome transmission fidelity mutants in *Saccharomyces cerevisiae*. *Genetics* 124, 237–249.
- Sriramachandran AM, Dohmen RJ (2014). SUMO-targeted ubiquitin ligases. *Biochim Biophys Acta* 1843, 75–85.
- Takahashi Y, Toh-e A, Kikuchi Y (2001). A novel factor required for the SUMO1/Smt3 conjugation of yeast septins. *Gene* 275, 223–231.
- Takahashi Y, Toh EA, Kikuchi Y (2003). Comparative analysis of yeast PIAS-type SUMO ligases *in vivo* and *in vitro*. *J Biochem* 133, 415–422.
- Tomonaga T, Matsushita K, Yamaguchi S, Oohashi T, Shimada H, Ochiai T, Yoda K, Nomura F (2003). Overexpression and mistargeting of centromere protein-A in human primary colorectal cancer. *Cancer Res* 63, 3511–3516.
- Ulrich HD (2009). The SUMO system: an overview. *Methods Mol Biol* 497, 3–16.
- van de Pasch LA, Miles AJ, Nijenhuis W, Brabers NA, van Leenen D, Lijnzaad P, Brown MK, Ouellet J, Barral Y, Kops GJ, et al. (2013). Centromere binding and a conserved role in chromosome stability for SUMO-dependent ubiquitin ligases. *PLoS One* 8, e65628.
- Verdaasdonk JS, Gardner R, Stephens AD, Yeh E, Bloom K (2012). Tension-dependent nucleosome remodeling at the pericentromere in yeast. *Mol Biol Cell* 23, 2560–2570.
- Wang Z, Prelich G (2009). Quality control of a transcriptional regulator by SUMO-targeted degradation. *Mol Cell Biol* 29, 1694–1706.
- Westerbeck JW, Pasupala N, Guillotte M, Szymanski E, Matson BC, Esteban C, Kerscher O (2014). A SUMO-targeted ubiquitin ligase is involved in the degradation of the nuclear pool of the SUMO E3 ligase Siz1. *Mol Biol Cell* 25, 1–16.
- Wieland G, Orthaus S, Ohndorf S, Diekmann S, Hemmerich P (2004). Functional complementation of human centromere protein A (CENP-A) by Cse4p from *Saccharomyces cerevisiae*. *Mol Cell Biol* 24, 6620–6630.
- Wu Q, Qian YM, Zhao XL, Wang SM, Feng XJ, Chen XF, Zhang SH (2012). Expression and prognostic significance of centromere protein A in human lung adenocarcinoma. *Lung Cancer* 77, 407–414.
- Xie Y, Rubenstein EM, Matt T, Hochstrasser M (2010). SUMO-independent *in vivo* activity of a SUMO-targeted ubiquitin ligase toward a short-lived transcription factor. *Genes Dev* 24, 893–903.